JOURNAL OF BACTERIOLOGY, Dec. 2003, p. 6841–6851 Vol. 185, No. 23
0021-9193/03/$08.00+0 DOI: 10.1128/JB.185.23.6841–6851.2003

Transcription of the Toxin Genes Present within the Staphylococcal Phage ϕSa3ms Is Intimately Linked with the Phage's Life Cycle

Paul Sumby† and Matthew K. Waldor*

Departments of Medicine and Microbiology, Tufts University School of Medicine and Howard Hughes Medical Institute, Boston, Massachusetts

Received 27 May 2003/Accepted 27 August 2003

ϕSa3ms, a lysogenic bacteriophage encoding the staphylococcal enterotoxins SEA, SEG, and SEK and the fibrinolytic enzyme staphylokinase (Sak), was identified in the unannotated genome sequence of the hypervirulent community-acquired *Staphylococcus aureus* strain 476. We found that mitomycin C induction of ϕSa3ms led to increased transcription of all four virulence factors. The increase in *sea* and *sak* transcription was a result of read-through transcription from upstream latent phage promoters and an increase in phage copy number. The majority of the *seg2* and *sek2* transcripts were shown to initiate from the upstream phage *cI* promoter and hence were regulated by factors influencing *cI* transcription. The lysogeny module of ϕSa3ms was shown to have some λ-like features with divergent *cI* and *cro* genes. Band shift assays were used to identify binding sites for both CI and Cro within the region between these genes, suggesting a mechanism of control for the ϕSa3ms lytic-lysogenic switch. Our findings suggest that the production of phage-encoded virulence factors in *S. aureus* may be regulated by processes that govern lysogeny.

Staphylococcus aureus is a leading cause of nosocomial and community-acquired infections worldwide (42). *S. aureus* causes a wide range of diseases that vary in severity from mild skin infections, such as boils and furuncles, to life-threatening diseases, like toxic shock syndrome and endocarditis. The ability of *S. aureus* to cause such a wide variety of diseases is thought to be due in part to its elaboration of a large number of secreted and cell-surface associated virulence factors (1, 5, 21, 36, 48).

Much of the variation between *S. aureus* strains appears to be attributable to mobile genetic elements, such as plasmids, bacteriophages, pathogenicity islands, transposons, insertion sequences, and the staphylococcal chromosomal cassette (2, 27). The bacteriophages and pathogenicity islands of *S. aureus* encode many virulence factors (35). The known phage-encoded virulence factors include Panton-Valentine leukocidins (24, 33), exfoliative toxin type A (47), and staphylococcal enterotoxins (SEs) (3). The SEs constitute a family of related proteins whose activities are associated with staphylococcal food poisoning, toxic shock syndrome, and possibly several autoimmune disorders (17, 41). SEs are powerful superantigens that activate subsets of T lymphocytes to liberate various cytokines, including gamma interferon and tumor necrosis factor (41). In addition to these characterized phage-encoded virulence factors, a number of putative *S. aureus* virulence factors, such as staphylokinase (Sak), are also encoded in phage genomes (25). Staphylokinase, a potent plasminogen activator, has been hypothesized to aid in the dissemination of *S. aureus* from fibrinous clots and abscesses (1).

The genome sequences of two *S. aureus* isolates derived from life-threatening community-acquired infections have been determined (2; unpublished data). The methicillin-resistant strain MW2 (sequenced at Juntendo University, Tokyo, Japan) was isolated in 1998 from North Dakota after it caused septic arthritis and fatal septicemia in a 16-month-old girl (2). Methicillin-sensitive strain MSSA476 (sequenced at the Sanger Institute, Cambridge, United Kingdom) was isolated in 1998 from Oxford, United Kingdom after it caused osteomyelitis and bacteremia in a 9-year-old boy. By mining the unannotated MSSA476 genome for phage-like sequences, we identified a prophage that encodes the previously characterized enterotoxins SEA, SEG, and SEK and the fibrinolytic enzyme Sak. Here we describe and characterize this phage, designated ϕSa3ms, from MSSA476.

Although the physical linkage of *S. aureus* virulence factors with phage genomes has been recognized for almost two decades (3), it is not known whether the life cycles of the phages influence the expression of the virulence genes and thus *S. aureus* pathogenicity. Here we show that upon ϕSa3ms prophage induction, transcription of *sea*, *seg2*, *sek2*, and *sak* are greatly increased. Phage-encoded factors were found to be required for the increases in *sea* and *sak* transcription. Interestingly, the majority of *seg2* and *sek2* transcripts initiated from the upstream ϕSa3ms repressor (*cI*) promoter, indicating that factors that influence *cI* transcription also influence virulence gene expression. Finally, the location of the putative CI and Cro binding sites suggests a potential mechanism for regulation of ϕSa3ms lysogeny and hence virulence factor expression.

MATERIALS AND METHODS

Bacterial strains and plasmids. A list of the bacterial strains and plasmids used in this study is shown in Table 1. *Escherichia coli* strains were grown in Luria-Bertani broth with ampicillin (100 μg/ml). *S. aureus* strains were grown in Todd-Hewitt broth (Difco) containing 0.2% (wt/vol) yeast extract (Difco) (THY) or in trypic soy broth (TSB) (Becton Dickinson) as indicated below; media were supplemented with 10 μg of chloramphenicol per ml when appropriate.

* Corresponding author. Mailing address: Tufts Medical School, Department of Microbiology, 136 Harrison Ave., Boston, MA 02111. Phone: (617) 636-2730. Fax: (617) 636-2723. E-mail: matthew.waldor@tufts.edu.

† Present address: Laboratory of Human Bacterial Pathogenesis, Rocky Mountain Laboratories, National Institute of Allergy and Infectious Diseases, National Institutes of Health, Hamilton, MT 59840.

TABLE 1. Bacterial strains and plasmids used in this study

Strain or plasmid	Description	Source or Reference
S. aureus strains		
MSSA476	Wild type	Sanger Centre
RN4220	Proficient in DNA uptake via transformation	26
MS79	MSSA476 (ϕSa3ms *ror*::pPS79)	This study
E. coli strains		
XL1-Blue	*recA1 endA1 gyrA96 thi-1 hsdR17 supE44 relA1 lac* [F′ *proAB lacI*^{q}ZΔM15 Tn*10* (Tet^r)]	Stratagene
DH5α	*recA1 endA1 gyrA96 thi-1 hsdR17 supE44 relA1* Δ*lacU169* (ϕ80 *lacI*^{q}ZΔM15)	
Plasmids		
pBT9	*E. coli-S. aureus* shuttle vector (Ts in *S. aureus*), Cm^r in *S. aureus*, Amp^r in *E. coli*	12
pPS79	pBT9 containing internal fragment of ϕSa3ms *ror*	This study
pQE-60	Six-His *E. coli* expression vector, Amp^r	Qiagen
pCROX	pQE-60 containing ϕSa3ms *cro*	This study
pCIX	pQE-60 containing ϕSa3ms *cI*	This study

Bioinformatic analyses. The currently unannotated MSSA476 genome sequence (produced by the *S. aureus* Sequencing Group at the Sanger Institute and available at www.sanger.ac.uk/Projects/S_aureus/) was mined for phage-like sequences by performing BLAST searches (available at www.ncbi.nlm.nih.gov/BLAST/) by using known phage-associated sequences, including sequences encoding SEs and integrases. Overlapping regions of interest were obtained from the FTP site, and putative open reading frames (ORFs) were identified by using Frameplot 3.0beta (available at www.nih.go.jp/~jun/cgi-bin/frameplot-3.0b.pl). BLAST searches were then performed with these putative ORFs to identify orthologues. The method of Dodd and Egan (18) was used to identify putative helix-turn-helix motifs, and possible N-terminal signal sequences were identified by using SignalP V2.0.b2 (available at www.cbs.dtu.dk/services/SignalP-2.0/). Protein sequences were scanned for sites or signatures against the PROSITE database by using PROSCAN (available at http://npsa-pbil.ibcp.fr). Conserved domains were identified using the National Center for Biotechnology Information conserved domain search program (available at www.ncbi.nlm.nih.gov/Structure/cdd/cdd.shtml).

Construction of a *ror* null mutant. PCR primers were created to amplify a central region of *ror* (5′-GCGGATCCTGGCTATTTAAAGAAAAGAG-3′ and 5′-GCCTGCAGACATGAGGTTTGTATGTTTG-3′), which was cloned directly into pBT9 after restriction digestion of the PCR products at the sites underlined in the primers, creating plasmid pPS79. pBT9 is an *E. coli-S. aureus* shuttle vector that is temperature sensitive for replication in *S. aureus* (12). pPS79 was introduced into the restriction-deficient *S. aureus* strain RN4220 by transformation as previously described (28). pPS79 was then transduced from RN4220 into MSSA476 by using phage 80α as previously described (34). Single crossovers were selected by inoculating 2 ml of TSB containing chloramphenicol with a single colony and incubating the culture for 8 h at 42°C before streaking it onto TSA plates containing chloramphenicol. The plates were then incubated at 42°C overnight. The presence of *ror*::pPS79 was confirmed by Southern blotting (data not shown). One caveat of this approach is that MS79 (*ror*::pPS79) must be grown at 42°C to maintain the integrated form of the plasmid. Therefore, in all experiments in which MS79 was utilized, both this strain and wild-type strain MSSA476 were streaked and grown overnight at 42°C. However, after appropriate dilution of overnight cultures, additional incubation was carried out at 37°C. In each experiment an MSSA476 control which had been grown exclusively at 37°C was also included. In all cases there was no difference between the results for MSSA476 grown at 37°C and the results for MSSA476 grown at 42°C.

RNA extraction and Northern blotting. Total RNA was isolated from *S. aureus* cultures by using Qiagen RNeasy mini kits (Qiagen, Valencia, Calif.) as recommended by the manufacturer, except that lysostaphin was substituted for lysozyme. Overnight TSB cultures were diluted 1:200 (see Fig. 2) or 1:400 (see Fig. 4) into fresh TSB and grown with shaking at 37°C to an optical density at 600 nm of 0.1 (see Fig. 2) or 0.14 (see Fig. 4) before extraction of RNA from aliquots (time zero). Each culture was then split into two parts, and mitomycin C was added to one of the parts at a final concentration of 0.3 μg/ml. The cultures were then incubated at 37°C, and RNA was extracted from aliquots of both cultures at several subsequent times. Total RNA was quantified by spectrophotometric analysis (optical density at 260 nm), and equal amounts of RNA were used for Northern blotting performed by using the Ambion NorthernMax-Gly protocol (Ambion, Austin, Tex.). Probes for Northern blotting were created by using an Ambion Strip-EZ kit.

Genomic DNA extraction and Southern blotting. Genomic DNA was isolated as previously described (34). Southern blotting was performed by using standard techniques, and the blots were probed with horseradish peroxidase-labeled probes generated by using an Amersham ECL direct labeling kit (Amersham, Little Chalfont, Buckinghamshire, England).

Phage DNA isolation. Phage DNA was isolated from supernatants of MSSA476 cultures as previously described (23). Isolated phage DNA was subjected to restriction analysis and separated on standard agarose gels stained with ethidium bromide.

Single-plaque purification of phage and plaque lifts. Single plaques were isolated by seeding 3 ml of soft THY (supplemented with 5 mM $CaCl_2$) with 10 μl of an overnight RN4220 culture and overlaying the resulting culture onto a plate containing THY (supplemented with 5 mM $CaCl_2$) spread with dilutions of MSSA476 culture supernatants. Plaque lifting was performed by using standard procedures after incubation of the plates for 18 h at 37°C.

Identification of transcriptional start sites by 5′-RACE. The Invitrogen 5′ rapid amplification of cDNA ends (RACE) system (Invitrogen, Carlsbad, Calif.) was used to identify putative transcriptional start sites for *cI* and *cro* according to the manufacturer's instructions. The following primers were used for these assays: CRORA (5′-TTGTTCCATTGTGTCCCTCC-3′), CROXR (5′-CGGGATCCTATAACATGAACTTTTTC-3′), MSREP2 (5′-GCGAATTCTCACTGTCTTTCCAACCAAC-3′), CISF (5′-CCACATGCAATATACGATAC-3′), and SEQR (5′-GAGTAGAAACTTTGTCTGTAG-3′). Briefly, primer SEQR or CRORA was added to total RNA isolated from MSSA476 and used to prime first-strand cDNA synthesis with reverse transcriptase. A poly(C) 3′ tail was added to the cDNA by using terminal transferase, and each of the tailed cDNAs was used as template in a PCR performed with a downstream primer (relative to the directions of the SEQR and CRORA primers) and a primer that ended with a poly(G) sequence (primer AAP; Invitrogen). Control PCRs in which nontailed cDNAs were used as templates were used as controls for AAP primer specificity. Products were visualized on standard agarose gels stained with ethidium bromide. Bands were excised from the gels by using a Qiagen gel extraction kit and were sequenced at the Tufts University School of Medicine Core Sequencing Facility.

Cloning and overexpression of CI and Cro genes. *cI* and *cro* were amplified by PCR by using primers CIXF (CGCCATGGGCCGCGAAAAAGTTTCAAATCGCCTTAAACAC) and CIXR (GCGGATCCCAATACAACTTTGCCCATTAC) for *cI* and CROXF (CGCCATGGGCTGTTACGACTACTCACGTTTG) and CROXR (CGGGATCCTATAACATGAACTTTTTC) for *cro*. The PCR products were cloned into the *E. coli* expression vector pQE-60 (Qiagen), creating pCIX and pCROX, respectively. To enable cloning into pQE-60, the PCR primers for amplifying both *cI* and *cro* contained an *Nco*I site overlapping the start codon and a *Bam*HI site at the 3′ end of the gene. Ligation of the *Nco*I-*Bam*HI-digested PCR products into pQE-60 generated a six-His tag at the C terminus of each expressed protein. Proteins were expressed in *E. coli* strain XL1-Blue following standard isopropyl-β-D-thiogalactopyranoside (IPTG) induction. Proteins were purified on Ni-agarose columns (Qiagen) by following the manufacturer's instructions.

Band shift assays. Three probes were generated by PCR by using 5′-radiolabeled primers. Probe 1 was a 147-bp region of ϕSa3ms from the region between ORFs 49 and 50 and contained a putative CI binding half-site (primers 5′-CATCTACAACTTTATCTTGC-3′ and 5′-AGTTGAACGTGTTGATGATG-3′);

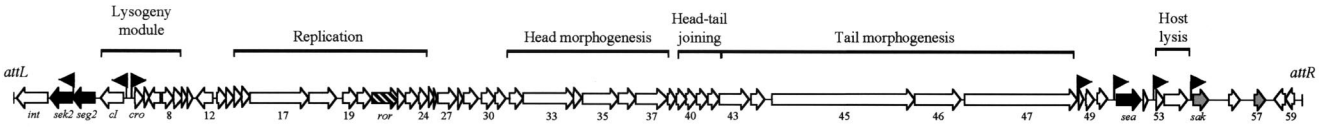

FIG. 1. Genetic organization and ORF map of the 42,612-bp ϕSa3ms genome. Putative ORFs are indicated by arrows that show the directions of transcription. The raised arrows indicate the approximate locations of the promoters mapped in this study. Enterotoxin genes are indicated by solid arrows, while other putative virulence factors are indicated by gray arrows. *orf21*, designated *ror*, which was inactivated in this study, is indicated by a cross-hatched arrow. Groups of genes whose protein products are functionally interrelated are indicated above the ORF map.

probe 2 was a 99-bp region overlapping the 3′ end of *cro* and contained a complete CI binding site (primers 5′-TTGTTCCATTGTGTCCCTCC-3′ and 5′-ATACAACTACTAGATATACC-3′); and probe 3 was a 209-bp region overlapping the region between *cI* and *cro* and contained two complete putative CI binding sites and a single putative Cro binding site (primers 5′-TTTCTACTAT TTTCCCGCTC-3′ and 5′-CTCTCATTTAGTGCACCTCC-3′). After the primers were treated with kinase, unincorporated nucleotides were removed by using a MicroSpin G-25 column (Amersham). Unincorporated primers were removed after PCR by using a Qiagen PCR purification kit. Purified protein, either CI or Cro, was diluted in 1× binding buffer (20 mM Tris-HCl [pH 7.5], 1 mM $MgCl_2$, 5% glycerol, 50 μg of bovine serum albumin per ml); 50 ng of sonicated salmon sperm DNA per μl and 4 mM dithiothreitol were included in the binding reaction mixtures, which were incubated at room temperature for 10 min. Samples were loaded and run on Invitrogen 6% polyacrylamide retardation gels. The gels were dried and then exposed to BioMax MS film (Eastman Kodak Company, Rochester, N.Y.).

RESULTS

Identification and analysis of phage genomes within *S. aureus* MSSA476. Conserved phage genes (e.g., *int*) and known phage-encoded virulence genes (e.g., *sak*) were used to search the unfinished MSSA476 database (Sanger Institute) for phage-like sequences. Two putative phage genomes, designated ϕSa3ms and ϕSa4ms, were identified by this method. The designations chosen were based on the classification proposed by Baba et al. (2). ϕSa4ms most closely resembles ϕ12 from the prototypical *S. aureus* strain NCTC 8325 (22). However, unlike integration of ϕ12 in NCTC 8325, ϕSa4ms is integrated into the MSSA476 genome between the gene encoding a toxic anion resistance protein orthologue and an orthologue of *htrA*, which encodes a stress response serine protease implicated in the virulence of a number of pathogenic bacteria (15, 37). The *attB* site is located only 30 bases upstream of the *htrA* start codon, raising the possibility that ϕSa4ms integration and excision affect the transcription of *htrA*. Analysis of each individual ORF within ϕSa4ms failed to identify any known or putative virulence factors, similar to what has been reported for ϕ12 (22).

The ϕSa3ms genome is shown in Fig. 1. ϕSa3ms encodes the SEs SEA, SEG, and SEK, along with the putative virulence factors SAK and a protein (Orf57) thought to be involved in expression of a fibrinogen binding protein (4, 22). Remarkably, ϕSa3mw, a phage recently identified in the community-acquired methicillin-resistant *S. aureus* strain MW2 (2), differs from ϕSa3ms at only 14 bp over the entire 42,612-bp genome. The 14 bp of sequence divergence results in silent mutations at four sites, single amino acid changes in the Sak, amidase, Orf49, tail, portal, and integrase proteins, and a 4-bp deletion within a putative antirepressor gene resulting in a truncated product in ϕSa3ms compared to the ϕSa3mw product. The 4-bp deletion in ϕSa3ms was shown to be authentic and not a result of a sequencing error by resequencing this region of ϕSa3ms (data not shown).

Table 2 shows the closest homologue of each ϕSa3ms ORF identified by BLASTP searches of the GenBank database (to be more informative, ϕSa3mw hits were omitted). Remarkably, the sequence encoded by every ϕSa3ms ORF exhibited at least 90% amino acid identity to the sequences encoded by ORFs in other double-stranded DNA tailed *S. aureus* phages.

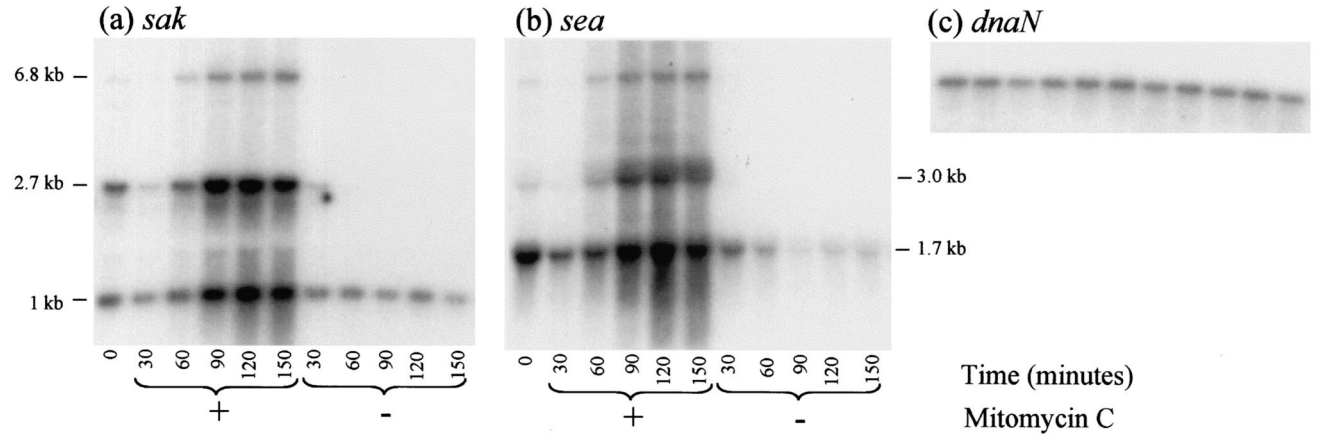

FIG. 2. Treatment with the prophage-inducing agent mitomycin C increases *sak* and *sea* transcript levels. Mitomycin C (300 ng/ml) was added to one of two identical MSSA476 cultures, and RNA was extracted from both cultures every 30 min for 2.5 h. Six micrograms of total RNA was loaded in each lane and subsequently probed with *sak* (a), *sea* (b), or *dnaN* (c). The *dnaN* blot acted as a control for RNA loading.

TABLE 2. Putative ORFs in ϕSa3ms

ORF (gene)	Coding region[a]	Probable function or motifs[b]	% Identity (no. of amino acids)[c]	Homology[d]	
				Gene	Source
1 (*int*)	139–1176[e]	Integrase	99 (345)	*int*	ϕ42
2 (*sek2*)	1260–1988[e]	Enterotoxin	97 (241)	*sek*	SaP13
3 (*seg2*)	2012–2740[e]	Enterotoxin	98 (242)	*entQ*	SaP11
4 (*cI*)	2936–3706[e]	Repressor (cl-like)	100 (256)	*orf31*	ϕPVL
5 (*cro*)	3865–4089	Repressor (cro-like)	100 (74)	*orf4*	ϕ13
6	4086–4367	Regulatory	98 (93)	*orf5*	ϕ13
7	4391–4930[e]	Unknown	100 (179)	*suv1995*	ϕN31
8	4987–5379	Anti-repressor (C terminus truncated)	99 (130)	*orf7*	ϕ13
9	5381–5732	Anti-repressor (N terminus truncated)	100 (117)	*orf7*	ϕ13
10	5748–5945	Unknown	100 (65)	*sav1993*	ϕN315
11	5976–6116	Unknown	95 (46)	*orf8*	ϕPV83
12	6131–6763[e]	Unknown	100 (211)	*sav1992*	ϕN315
13	6822–7142	Conserved, unknown	100 (106)	*sav1991*	ϕN315
14	7139–7300	Signal sequence	100 (53)	*orf9*	ϕ13
15	7393–7653	Replication (unknown)	100 (86)	*orf10*	ϕ13
16	7662–7925	Unknown	100 (87)	*sav1987*	ϕN315
17	7928–9877	ATP/GTP binding (replication)	98 (647)	*sav1986*	ϕN315
18 (*rec7*)	9879–10799	Recombination	100 (306)	*sav1985*	ϕN315
19	11012–11497	Metal-dependent hydrolase (β-lactamase superfamily 1)	97 (161)	*sav1984*	ϕN315
20 (*ssb*)	11498–11968	Single-strand binding protein	96 (156)	*sal792*	ϕN315
21 (*ror*)	11998–12891	Replisome organizer	97 (297)	*saI791*	ϕN315
22	12898–13116	DNA ligase	98 (72)	*saI790*	ϕN315
23 (*rus*)	13125–13529	Holliday junction resolvase	91 (134)	*sav1980*	ϕN315
24	13542–13856	Unknown	90 (95)	*saI788*	ϕN315
25 (*rinB*)	13870–14019	*int* expression	100 (49)	*sas062*	ϕN315
26	14019–14171	Serine protease	100 (50)	*orf58*	ϕPVL
27	14178–14828	Unknown	100 (216)	*orf59*	ϕPVL
28	14828–15028	Signal sequence	98 (66)	*orf33*	ϕPV83
29	15051–15521	Unknown	99 (133)	*orf61*	ϕPVL
30	15636–16088	Unknown	99 (150)	*orf62*	ϕPVL
31	16104–16448	HNH nuclease	100 (114)	*orf63*	ϕPVL
32	16577–17044	Terminase small subunit	100 (155)	*orf1*	ϕPVL
33	17047–18741	Terminase large subunit	100 (564)	*orf38*	ϕPV83
34	18755–18955	Signal sequence	98 (66)	*orf39*	ϕPV83
35	18961–20211	Portal protein	99 (416)	*orf4*	ϕPVL
36	20204–20788	Prohead protease	100 (194)	*orf41*	ϕPV83
37	20876–22123	Head	99 (415)	*orf42*	ϕPV83
38	22159–22317	Unknown	100 (52)	*orf43*	ϕPV83
39	22326–22658	DNA packaging	100 (109)	*orf44a*	ϕPV83
40	22645–22980	Head-tail joining	100 (110)	*orf10*	ϕPVL
41	22980–23357	Head-tail joining	100 (125)	*orf47*	ϕPV83
42	23354–23734	Head-tail joining	99 (126)	*orf38*	ϕ13
43	23735–24688	Tail with immunoglobulin-like domain 2	100 (317)	*orf39*	ϕ13
44	24752–25199	Unknown	100 (148)	*orf40*	ϕ13
45	25437–30086	Tape measure	98 (1,550)	*orf41*	ϕ13
46	30086–31576	Unknown	96 (496)	*orf42*	ϕ13
47	31592–35374	Tail	99 (1,260)	*savI953*	ϕN315
48	35367–35519	Unknown	100 (50)	*savI952*	ϕN315
49	35565–35852	Unknown	100 (95)	*savI951*	ϕN315
50	35908–36282	Transmembrane region	100 (124)	*savI950*	ϕN315
51 (*sea*)	36655–37428	Enterotoxin	100 (257)	*sep*	ϕN315
52	37579–37713	Unknown	100 (44)	*savI947*	ϕN315
53	37925–38179	Holin	100 (84)	*savI946*	ϕN315
54	38191–38946	Amidase	99 (251)	*orf47*	ϕ13
55 (*sak*)	39137–39628	Staphylokinase	100 (163)	*sak*	ϕN315
56	40318–40614	Truncated amidase	100 (98)	*'lytA*	ϕN315
57	41126–41476	*fib* expression (signal sequence)	100 (116)	*savI942*	ϕN315
58	41768–42076[e]	Unknown	99 (94)	*saI753*	ϕN315
59	42100–42279[e]	Unknown	100 (59)	*savI940*	ϕN315

[a] Nucleotide positions from the start codon to the stop codon.
[b] Motifs and potential functions were determined by bioinformatic analysis as described in Materials and Methods.
[c] Level of amino acid identity between each ORF and the best hit, excluding ϕSa3mw ORFs (number of amino acids over which identity exists).
[d] The best hit (excluding ϕSa3mw ORFs) as determined by BLASTP analysis and its source.
[e] Transcription occurs on the complementary strand (from right to left in Fig. 1).

The extensive similarity of ϕSa3ms sequences to the sequences found in other phages presumably reflects recombination among several other phages that occurred during the evolutionary history of ϕSa3ms (20). As is typical for phage genomes, ϕSa3ms genes with similar functions are clustered together (Fig. 1). The putative ϕSa3ms lysogeny module consists of divergent *cI* and *cro* homologues, suggesting that there is a mechanism for control of the lysogenic-lytic decision similar to the mechanism in λ. The putative replication module includes homologues of genes encoding the recombination protein RecT, the Holliday junction resolvase Rus, a single-stranded binding protein, a DNA ligase (ORF 22), and the putative replisome organizer Ror (Table 2). ORF 21 was designated *ror* after BLASTP analysis identified the origin-binding Ror protein from *Bacillus subtilis* phage SPP1 as the highest-scoring homologue with a defined function (32, 38). Further evidence that Ror has a role in replication was obtained from a National Center for Biotechnology Information conserved domain search analysis that revealed that Ror is similar to the PriA primosome component DnaD (31). The head morphogenesis region contains two terminase subunits, a characteristic of phages that package their genomes via a head-full mechanism (*pac*-type phage) (29). ORF 31 encodes a putative homing nuclease based on the similarity of the protein to a number of endonucleases belonging to the HNH family (16). The putative head-tail joining, tail morphogenesis, and host lysis regions are similar to those found in previously described *S. aureus* phages (22).

Integration of ϕSa3ms disrupted the β-hemolysin gene of MSSA476. Such negative conversion of a potential virulence gene has been observed after integration of a number of *S. aureus* phages (14). Studies of the regulation of integration and excision of *S. aureus* phages have identified either *xis* homologues or an ORF adjacent to the integrase gene termed ORFC, which is thought to function like *xis* and facilitate phage excision (13). However, no such gene is present upstream of the putative ϕSa3ms *int* gene, raising the question of how ϕSa3ms integration and excision are controlled. ϕSa3ms, like all previously described *S. aureus* phages, contains a conserved hairpin loop upstream of *int* (13). A number of *S. aureus* phages also contain a second conserved hairpin sequence upstream of *int* (22). These putative hairpin sequences have been hypothesized to be important in *int* gene regulation (13, 22). The putative hairpin sequence identified by Carroll and colleagues (13) even occurs upstream of both the staphylococcal pathogenicity island 1 (SaPI1) and SaPI3 *int* genes.

Both ϕSa3ms and ϕSa4ms form phage particles. We initially examined whether ϕSa3ms and ϕSa4ms were defective prophages by assaying supernatants of mitomycin C-treated MSSA476 cultures for the presence of phage DNA. After the isolated phage DNA was subjected to restriction analysis, bands of the expected sizes for ϕSa3ms and ϕSa4ms DNA were detected at nearly equal intensities (data not shown). Southern blot analysis of isolated phage DNA performed with a ϕSa3ms-specific *sea* probe provided further evidence that ϕSa3ms was capable of producing phage particles (data not shown). No hybridizing signal was observed when a chromosomally encoded gene was used as a probe (data not shown). Single-plaque purification of phage derived from mitomycin C-treated MSSA476, followed by DNA isolation and restriction analysis, revealed that while ϕSa4ms was capable of producing infectious particles (plaques), no ϕSa3ms plaques were observed (data not shown). Plaque lift assays with the *sea* probe were also negative, suggesting either that ϕSa3ms produces phage particles that are noninfectious, that the indicator strain RN4220 lacks the necessary ϕSa3ms receptor, or that the conditions used were not conducive for ϕSa3ms infection.

Prophage induction greatly increases transcription of *sea* and *sak* from their native promoters and from upstream latent phage promoters. Northern blot analyses of RNA isolated from MSSA476 cultures at various times after mitomycin C treatment were carried out to investigate the effects of prophage induction on *sea* and *sak* transcript levels. In the absence of mitomycin C, a single approximately 1.0-kb *sak* transcript was present at relatively constant levels during the course of the experiment (Fig. 2). The levels of the single ~1.7-kb *sea* transcript in uninduced cultures also remained relatively constant during the experiment (Fig. 2). The 1.7-kb transcript likely originated from a previously characterized promoter immediately upstream of *sea* (8). Ninety minutes after mitomycin C treatment there were marked increases in both the 1.7-kb *sea* and 1.0-kb *sak* transcripts (Fig. 2). Mitomycin C treatment also resulted in the production of two higher-molecular-weight mRNAs for both genes (Fig. 2). The fact that the highest-molecular-weight bands for both *sea* and *sak* were the same size (approximately 6.8 kb), as well as the relative organization of these two genes in the ϕSa3ms genome, suggested that the 6.8-kb mRNA encodes both virulence factors.

Reprobing these Northern blots with a series of probes specific for genes 5′ of *sea* (*orf47*, *orf49*, and *orf50*) established that the 6.8-kb transcript likely initiates from a region between *orf47* and *orf49* (data not shown). The likely start site of the 3-kb *sea* transcript also mapped to this region. A probe for the ϕSa3ms holin gene showed that the 2.7-kb transcript containing *sak* originates 5′ of the phage holin gene (data not shown). These data confirm that *sea* and *sak* are expressed from their own promoters in uninduced cultures. However, following prophage induction, previously repressed phage promoters become active and contribute to increased *sea* and *sak* expression. To our knowledge, this is the first demonstration that there is linkage between prophage induction and increased virulence factor transcription in *S. aureus*.

ϕSa3ms replication contributes to mitomycin C induction of *sea* and *sak* transcription. At least two processes may contribute to the large increases in the amounts of the *sea* and *sak* transcripts observed after mitomycin C treatment of MSSA476. First, the data presented above suggest that mitomycin C treatment leads to activation of latent prophage promoters that can initiate transcription of *sea* and *sak*. Second, mitomycin C treatment likely leads to ϕSa3ms excision and replication, thereby increasing the amount of phage DNA template available for transcription. A replication-deficient ϕSa3ms prophage was constructed (Fig. 3) to investigate the contribution of ϕSa3ms replication to *sea* and *sak* transcription. To construct the replication-deficient prophage, we insertionally inactivated the putative replisome organizer (*ror*) gene through homologous recombination with pPS79 (Fig. 3a), a conditionally replication-defective plasmid containing a 719-bp internal fragment of *ror*.

Southern blot analyses revealed that mitomycin C treatment of MSSA476 resulted in a large increase in the ϕSa3ms copy

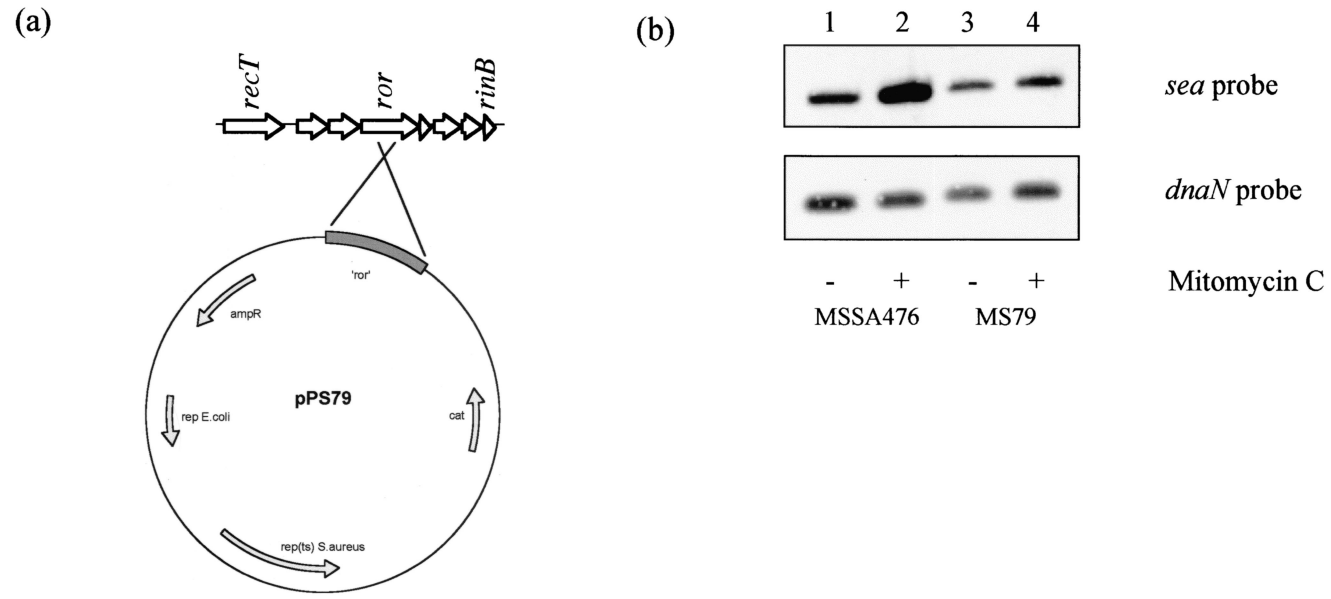

FIG. 3. Creation of replication-deficient ϕSa3ms. (a) An internal fragment of *ror* was cloned into the temperature-sensitive shuttle vector pBT9, creating pPS79, and used to insertionally inactivate *ror* through plasmid integration into the MSSA476 chromosome. (b) Southern blot analysis comparing the amounts of ϕSa3ms DNA (*sea* probe) and chromosomal DNA (*dnaN* probe) in MSSA476 and MS79 (*ror*::pPS79) in the absence and presence of mitomycin C.

number, as indicated by the increased intensity of the *sea* hybridizing band (Fig. 3b, lanes 1 and 2). A probe for a chromosomal gene, *dnaN*, was used as a loading control for these experiments. Insertional inactivation of *ror* in MS79 eliminated the increase in ϕSa3ms replication seen after mitomycin C treatment (Fig. 3b, lanes 3 and 4). These results demonstrate that mitomycin C treatment leads to ϕSa3ms replication and that pPS79 integration into *ror* eliminates ϕSa3ms replication.

In marked contrast to the pronounced increases in *sea* and *sak* transcription in MSSA476, there were no detectable increases in *sea* or *sak* transcription after mitomycin C treatment of MS79 cultures (Fig. 4), suggesting that ϕSa3ms replication is critical for the enhanced *sea* and *sak* transcription observed following prophage induction. An alternative explanation is that the integration of pPS79 into *ror* blocked the expression of an activator of *sea* and *sak* transcription. The absence of any higher-molecular-weight *sea* or *sak* transcripts in mitomycin C-treated MS79 cultures suggests that in addition to the replication deficit in the MS79 ϕSa3ms mutant, activation of latent phage promoters does not occur in this background. The

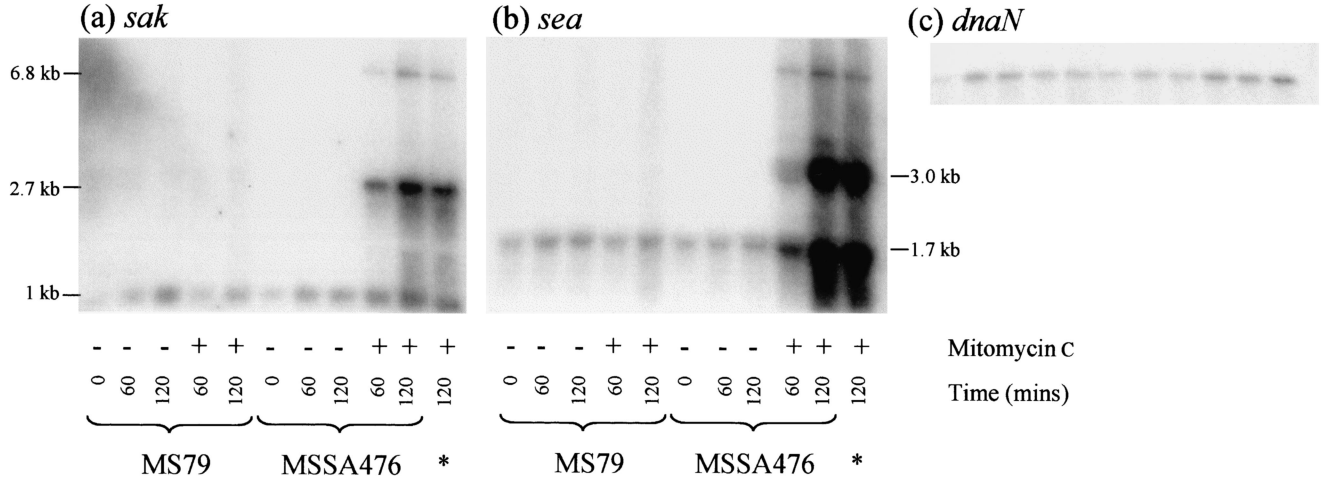

FIG. 4. Mitomycin C does not induce *sak* and *sea* transcription in MS79. Northern blots containing 5 μg of total RNA per lane were probed with *sea* (a), *sak* (b), or *dnaN* (c). The *dnaN* blot acted as a control for RNA loading. The lane indicated by an asterisk contained RNA from MSSA476 that was grown exclusively at 37°C to show that initial growth of this strain at 42°C had no effect on the subsequent transcription profiles of *sea* and *sak*.

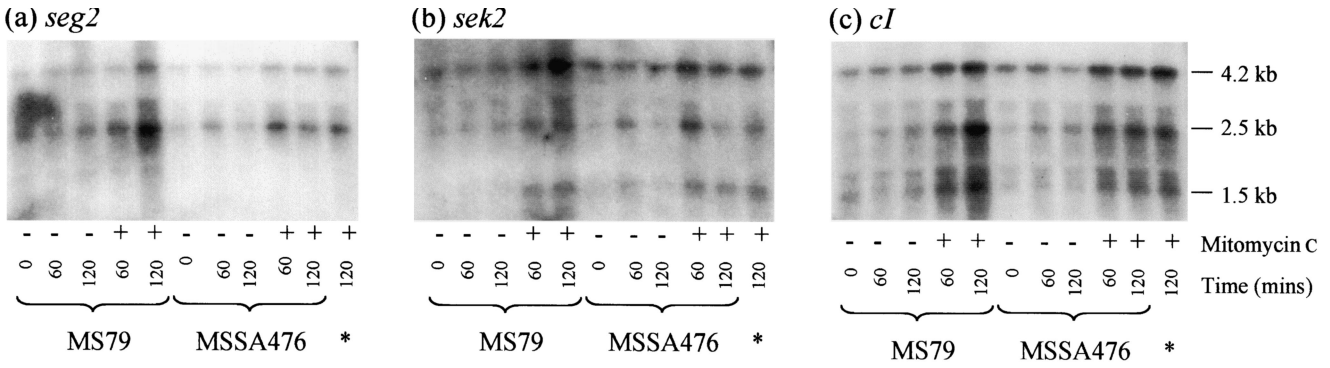

FIG. 5. Enterotoxin genes *seg2* and *sek2* are cotranscribed with the ϕSa3ms repressor gene *cI*. The Northern blot shown in Fig. 4 was stripped and reprobed with either *seg2* (a), *sek2* (b), or *cI* (c).

relative contributions of replication and latent phage promoter activation to the increases in *sea* and *sak* transcription that accompany prophage induction cannot be determined from analysis of MS79. Presumably, both processes contribute to the increases in *sea* and *sak* transcription that occur upon ϕSa3ms induction.

ϕSa3ms induction leads to increases in *seg2 and sek2* transcripts. We also investigated whether mitomycin C treatment of MSSA476 affected the levels of *seg2* and *sek2* transcripts. The direction of transcription of these two virulence factors is opposite the direction of transcription of *sea* and *sak*, and *seg2* and *sek2* are located at the opposite end of the ϕSa3ms prophage (Fig. 1). Two *seg2* hybridizing species and three *sek2* hybridizing species were detected in Northern blots of RNA isolated from uninduced MSSA476 cultures (Fig. 5a and b). Addition of mitomycin C to MSSA476 cultures increased the levels of all hybridizing species of both *seg2* and *sek2* (Fig. 5), although the magnitude of the increase was not as great as the magnitude of the increase observed with *sea* and *sak*. Unlike the lack of an effect of mitomycin C on *sea* and *sak* transcription in MS79, mitomycin C treatment elevated *seg2* and *sek2* transcript levels to similar degrees in MS79 and MSSA476 (Fig. 5a and b). These findings suggest that the levels of *seg2* and *sek2* expression are not influenced by phage replication or latent promoter activation.

The Northern blots probed with *seg2* and *sek2* probes both showed that 4.2- and 2.5-kb hybridizing fragments were present (Fig. 5a and b). This observation, along with the fact that *seg2* and *sek2* are adjacent and are transcribed in the same direction, suggested that these two transcripts contain both enterotoxin genes. Since both genes together span only ~1.6 kb, these two transcripts are also likely to include either the upstream *cI* gene or the downstream *int* gene (or both in the case of the 4.2-kb mRNA). To investigate these possibilities, the Northern blots described above were stripped and reprobed with a *cI* probe. As shown in Fig. 5c, 2.5- and 4.2-kb *cI*-encoding

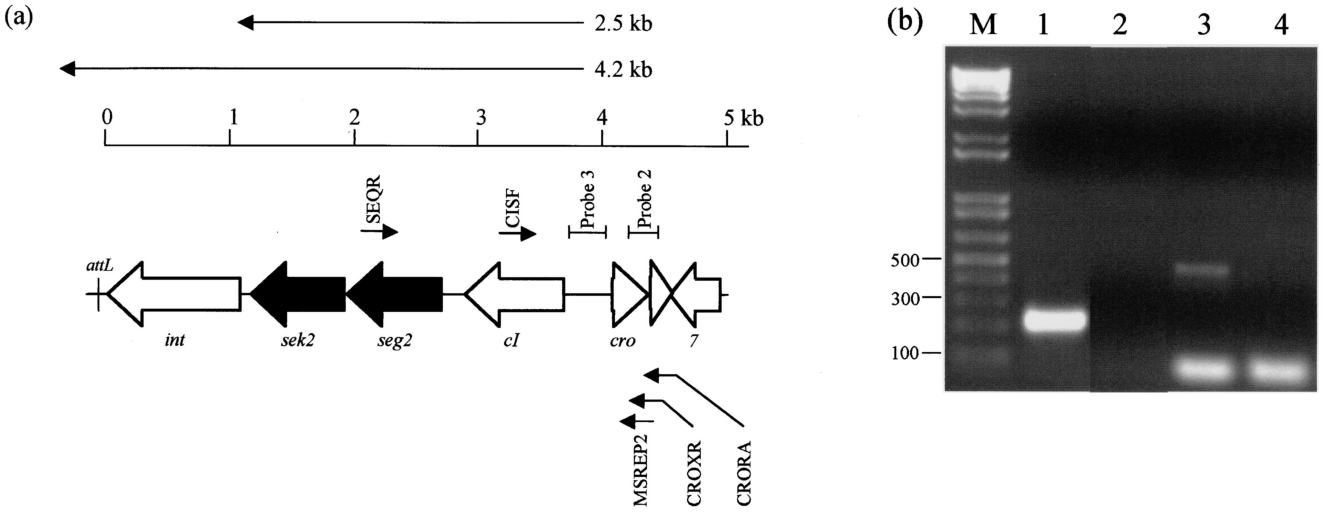

FIG. 6. 5′ RACE analysis of *cro* and *seg2* transcription start sites. (a) Physical map showing the organization of the left end of ϕSa3ms. The relative positions of the primers used in the gel shown in panel b are indicated, as are the positions of the 2.5- and 4.2-kb transcripts (Fig. 5) and probes 2 and 3 (Fig. 8). CRORA and SEQR were used in reverse transcription reactions to create *cro* and *seg2-cI* cDNA, respectively. (b) Ethidium bromide-stained gel showing the products of 5′ RACE reactions. Lanes 1 and 2, PCRs performed with primers MSREP2 and AAP with *cro* cDNA as the template (tailed in lane 1 and not tailed in lane 2); lanes 3 and 4, PCRs performed with primers CISF and AAP with *seg2-cI* cDNA as the template (tailed in lane 3 and not tailed in lane 4); lane M, DNA size marker.

FIG. 7. Locations of putative CI and Cro binding sites with respect to the likely *cI* and *cro* transcriptional start sites and promoter regions. Coding sequences are indicated by gray type, and noncoding sequences are indicated by black type. The transcription start sites of the divergently transcribed *cI* and *cro* genes are indicated by boxes. Putative −10 and −35 promoter sequences are underlined. The putative Cro and CI inverted repeat binding sites are shaded and are below converging arrows, respectively.

mRNAs were detected, in addition to a new 1.5-kb transcript, suggesting that there is transcriptional coupling of *cI*, *seg2*, and *sek2*. To further investigate this, 5′ RACE was used to map the 5′ transcriptional start site of *seg2*. We found that cDNA synthesized with a primer within *seg2* (SEQR [Fig. 6a]) extended beyond the 5′ end of *cI* (Fig. 6b, lane 3), indicating that at least some of the transcription of *seg2* initiates upstream of *cI*. The three *cI* transcripts that were different sizes, all of which presumably initiate from the same site, could arise by inefficient termination, antitermination of RNA polymerase, or posttranscriptional RNA processing. The relative locations of the 4.2- and 2.5-kb transcripts are shown in Fig. 6a. The presence of a *sek2* transcript that does not contain *seg2* (the 1.5-kb transcript [Fig. 5b]) implies that there is a functional promoter upstream of *sek2*. Since these data show that the enterotoxin genes *seg2* and *sek2* are mostly transcribed from the upstream *cI* promoter, it follows that factors effecting transcription of *cI* also regulate *seg2* and *sek2* transcription.

Mapping the *cI* and *cro* transcription initiation sites. As induction of ϕSa3ms into the lytic cycle led to significant increases in *sea*, *sak*, *seg2*, and *sek2* transcription, we investigated the genetic switch controlling the ϕSa3ms lytic-lysogenic cycle. We concentrated on the ϕSa3ms *cI* and *cro* homologues, two critical mediators of the λ genetic switch (39). In λ, CI production results in establishment of lysogeny and repression of the majority of the λ genes. Conversely, λ Cro production results in repression of *cI* expression, derepression of phage-encoded genes, and induction of λ into lytic growth. As a first step toward understanding how the ϕSa3ms *cI* and *cro* homologues are regulated, we identified the putative transcriptional start sites of *cI* and *cro* by 5′ RACE. To identify the *cI* start site, the 450-bp PCR product discussed above (Fig. 6b, lane 3) was sequenced. The *cro* transcriptional start site was identified by sequencing the 200-bp PCR product from Fig. 6b, lane 1. Figure 7 shows the putative transcriptional start sites for *cI* and *cro* and their corresponding −10 and −35 promoter sequences. The −10 and −35 sequences are consistent with typical staphylococcal promoters (34).

CI and Cro binding sites are present in the region between *cI* and *cro*. Inspection of the sequence of the region between the divergent *cI* and *cro* genes resulted in identification of two different inverted repeat sequences that might serve as CI and/or Cro binding sites (Fig. 7). One inverted repeat sequence is present once at the 3′ end of *cro* and twice in the *cI-cro* intergenic region; since one of these sequences overlaps the putative *cro* promoter, it was a good candidate CI operator for repression of *cro* transcription. The putative Cro binding site occurs once in the ϕSa3ms genome and overlaps the −35 sequence of the *cI* promoter, again suggesting a mechanism of action, this time for Cro prevention of *cI* transcription.

ϕSa3ms CI and Cro were overexpressed and purified from *E. coli* as C-terminal His-tagged fusion proteins and tested for the ability to bind to different regions of the ϕSa3ms genome in band shift assays. CI bound to a region of the ϕSa3ms genome that contained a single copy of the putative CI binding site (probe 2) but did not bind to a region containing only a half-site from the *orf49-orf50* intergenic region (probe 1) (Fig. 8a). Probe 3 consisted of the *cI-cro* intergenic region and thus contained a single putative Cro binding site and two putative CI binding sites (Fig. 7). Figures 8b and c show that both CI and Cro bound to probe 3 but not to control probes lacking the corresponding inverted repeat sequences. Two different DNA-protein complexes were seen when either CI or Cro was incubated with probe 3. Since probe 3 contained two putative CI binding sites, sequential loading of CI complexes onto the probe could account for the observed pattern. As there was only a single putative Cro inverted repeat binding site in this probe, the presence of two shifted complexes suggests that Cro monomers may be able to bind to individual half-sites; alternatively there may be more than one sequence to which Cro binds in this region. Supershift experiments performed with an anti-His antibody (Fig. 8b and data not shown) confirmed that the shifted DNA protein complexes were due to CI or Cro binding.

DISCUSSION

Phage-encoded toxins were first recognized more than 50 years ago (19); however, very little is known about the biology and role in pathogenesis of the many phages that encode virulence factors. Here we identified and annotated a prophage genome in the incomplete genome of the methicillin-sensitive *S. aureus* strain MSSA476, an organism that has caused severe community-acquired *S. aureus* infections (Nick Day, personal communication). This phage, ϕSa3ms, contains three enterotoxin genes, *sea*, *seg2*, and *sek2*, along with a gene encoding the fibrinolytic enzyme staphylokinase. The 42,612-bp ϕSa3ms genome exhibits extensive similarity to the genomes of other *S. aureus*-derived bacteriophages. ϕSa3ms was inducible with mitomycin C, and its DNA was detected in supernatants of mitomycin C-treated MSSA476 cultures; however, we did not identify suitable conditions for infecting the nonlysogenic *S. aureus* strain RN4220.

Mitomycin C treatment of MSSA476 led to increased transcription of four ϕSa3ms-encoded virulence factors. In the absence of prophage induction, *sea* and *sak* were transcribed at low levels. Prophage induction with mitomycin C led to marked increases in the amounts of these transcripts, as well as the appearance of new *sea* and *sak* transcripts from activation of latent upstream phage promoters. Putative sites for the two latent phage promoters were determined. One site was upstream of the ϕSa3ms holin gene; the activation of this pro-

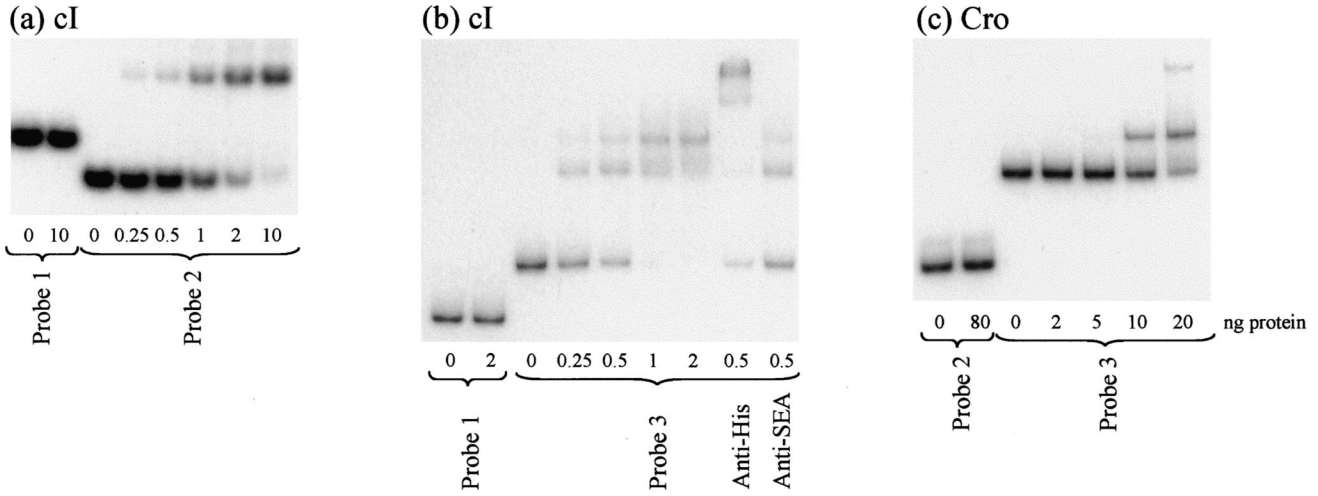

FIG. 8. ϕSa3ms CI and Cro specifically bind to specific regions of ϕSa3ms DNA. Bandshift assays were performed to test binding of purified C-terminal His-tagged CI (a and b) and Cro (c) to three ϕSa3ms-derived probes. Probe 1 was a 147-bp region of ϕSa3ms from the region between ORFs 49 and 50 that lacked the putative inverted repeat binding sites of CI and Cro. Probe 2 was a 99-bp region of ϕSa3ms that overlapped the 3′ end of *cro* and contained a single putative CI binding site (see Fig. 6a). Probe 3 was a 209-bp region of ϕSa3ms that overlapped the *cI-cro* intergenic region and contained two putative CI binding sites and one putative Cro binding site (see Fig. 6a). Anti-His antibody supershifted the cI-DNA binding complexes in panel b, whereas a negative control antibody (anti-SEA) did not.

moter led to transcriptional read-through of the downstream *sak* gene (2.7-kb mRNA in Fig. 2). The second promoter was in a region upstream of *orf*49 and downstream of *orf*47, the activation of which led to production of two virulence factor-encoding mRNAs, a 6.8-kb transcript containing both *sea* and *sak* and a 3-kb transcript containing only *sea* (Fig. 2). The mechanisms governing the production of transcripts of different sizes from these latent ϕSa3ms promoters are unknown. The possible mechanisms include inefficient termination, transcriptional antitermination, and RNA processing. An interesting observation from Fig. 2 is the presence of late gene phage-specific transcripts at time zero. This may be attributable to a stationary-phase-dependent decrease in prophage stability, as previously described for ϕLC3 in lactococci and P22 in *Salmonella enterica* serovar Typhimurium (30, 40). Evidence in support of this hypothesis comes from the lack of phage transcripts at time zero in Fig. 4, as the RNA for this analysis was isolated from cultures that had undergone a greater number of doublings.

The role of ϕSa3ms replication in virulence factor production was investigated by using MS79 (*ror*::pPS79). *ror* was chosen for insertional inactivation because the Ror homologue in *B. subtilis* phage SPP1 is essential for replication (38). In contrast to the transcript levels in MSSA476, the *sea* and *sak* transcript levels were not affected by mitomycin C treatment of MS79. While MS79 had a ϕSa3ms replication-deficient phenotype (Fig. 3b), the lack of ϕSa3ms lytic cycle transcripts (Fig. 4) suggests that activation of latent lytic cycle promoters does not occur in MS79. We hypothesize that the pPS79 integration in ϕSa3ms may have had a polar effect on expression of an activator (possibly *rinB*, which has a role in activation of *int* transcription in ϕ11 [49]) required for late gene transcription. As ϕSa3ms::pPS79 is defective both in replication and in transcriptional activation, the relative contributions of each of these factors to *sea* and *sak* transcription cannot be deciphered from analysis of MS79.

While the majority of *S. aureus* phage-encoded virulence factors are located downstream of phage lysis genes, ϕSa3ms and ϕSa3mw are unique due to the positions of virulence factors between the repressor and integrase genes of these phages. The increases in *seg2* and *sek2* transcription following prophage induction were less pronounced than the increases in *sea* and *sak* transcription. The majority of the *seg2* and *sek2* transcripts were found to initiate from the promoter upstream of the ϕSa3ms repressor gene *cI*, showing that *cI*, *seg2*, and *sek2* are part of an operon. The transcript sizes and the orientation of genes downstream of *cI* suggest that the 4.2-kb *cI* transcript also contains the downstream *int* gene. The identical transcriptional profiles of *cI*, *seg2*, and *sek2* from MSSA476 and MS79 cultures (Fig. 5) revealed that neither ϕSa3ms replication nor latent promoter activation plays a role in the transcription of these genes. Furthermore, these data suggest that factors which regulate *cI* transcription also regulate transcription of *seg2*, *sek2*, and *int*. Read-through transcription of SE genes and *int* from a repressor gene was suggested by the work of Yarwood and colleagues (48) in which they showed by microarray analysis that *int*, *seq*, and *sek* of SaPI3 have the same transcriptional profiles as the surrounding genes, with the first gene in the operon encoding a CI-like repressor (48). The constant transcription of *int* in a lysogen has important implications for the regulation of ϕSa3ms integration and excision.

Since the life cycle of ϕSa3ms determines transcription of its encoded virulence factors so dramatically, the putative lysogeny module of ϕSa3ms was analyzed. The ϕSa3ms CI and Cro proteins bound the region between the divergently transcribed *cI* and *cro* genes (Fig. 8), and the locations of the putative CI and Cro binding sites suggest that Cro binding prevents *cI* transcription and vice versa. This putative transcriptional re-

pression through CI or Cro binding may be similar to that described for phage λ (39). ϕSa3ms appears to differ from λ, however, by the presence of separate CI and Cro operator sequences and by the increase in ϕSa3ms *cI* expression that occurs after mitomycin C treatment. The latter observation is difficult to reconcile with the increases in *cro* levels that occur with prophage induction (data not shown). Further investigation is required to understand how the ϕSa3ms lytic switch functions; it appears that the molecular details of this switch differ from those of the λ switch.

The work described here showed that ϕSa3ms prophage induction leads to transcriptional up-regulation of four ϕSa3ms-encoded virulence factors. Whether the mitomycin C-stimulated increases in *sak*, *sea*, *seg2*, and *sek2* transcripts lead to increases in the levels of the corresponding proteins is currently unknown. However, the results of initial experiments exploring SEA production following mitomycin C treatment did not reveal parallel dramatic increases in SEA levels mirroring the increases observed in *sea* transcripts after ϕSa3ms induction (data not shown). Additional evidence in support of the idea that posttranscriptional regulation influences SEA production comes from the work of Borst and Betley (6–8), who suggested that factors in addition to *sea* mRNA levels affected SEA production.

The list of phage-encoded virulence factors continues to grow (for reviews see references 9 and 45) as the number of sequenced bacterial genomes expands. Lagging behind this expanding genomic information is an understanding of the biology of these prophages. Given the recent discovery that at least in one case phage biology can play an essential role in pathogenicity (45), this gap in our knowledge needs to be addressed. Studies with Shiga toxin-producing *E. coli* (44) and *Streptococcus pyogenes* (10) revealed that prophage induction leads to an increase in production of phage-encoded virulence factors. There is accumulating evidence that prophage induction occurs in vivo (11, 43, 44, 46), raising the possibility that host factors that promote prophage induction may play an important role in pathogenesis. The increased transcription of *sea* and *sak* upon prophage induction and the location of these genes interspersed with the lysis genes are similar to the increased transcription and location of the *stxAB* genes in Shiga toxin-producing *E. coli*. However, *seg2* and *sek2* differ from *stx* in both their location within the phage genome and in their level of transcriptional up-regulation upon phage induction. The different effects of ϕSa3ms induction on transcription of *sea* and *sak* and on transcription of *seg2* and *sek2* may be explained by their relative insertion sites in the ϕSa3ms genome. Insertion of *seg2* and *sek2* downstream of the repressor gene guarantees constitutive expression of these genes during lysogeny due to the absence of an efficient terminator downstream of *cI*, while the clustering of *sea* and *sak* with the ϕSa3ms lysis genes enables a burst of expression upon ϕSa3ms late gene transcription. It is tempting to speculate that the sites of insertion of virulence genes in phage genomes may be subject to selection that optimizes the phage control of expression of the genes for pathogenicity.

ACKNOWLEDGMENTS

We thank Tim Foster, John Iandolo, Jean Lee, and Kimberly Jefferson for strains and plasmids. We also thank the NEMC GRASP Digestive Disease Center for media, Anne Kane for purification of CI and Cro, Nick Day for information about MSSA476, and the Sanger Centre for release of the MSSA476 genome sequence before publication. Finally, we thank Harvey Kimsey and Anne Kane for critical comments on the manuscript.

This work was supported by NIH grant AI42347 and by the Howard Hughes Medical Institute.

REFERENCES

1. **Arvidson, S.** 2000. Extracellular enzymes, p. 379–385. *In* V. A. Fischetti, R. P. Novick, J. J. Ferretti, D. A. Portnoy, and J. I. Rood (ed.), Gram-positive pathogens. ASM Press, Washington, D.C.
2. **Baba, T., F. Takeuchi, M. Kuroda, H. Yuzawa, K. Aoki, A. Oguchi, Y. Nagai, N. Iwama, K. Asano, T. Naimi, H. Kuroda, L. Cui, K. Yamamoto, and K. Hiramatsu.** 2002. Genome and virulence determinants of high virulence community-acquired MRSA. Lancet **359:**1819–1827.
3. **Betley, M. J., and J. J. Mekalanos.** 1985. Staphylococcal enterotoxin A is encoded by phage. Science **229:**185–187.
4. **Boden, M. K., and J. I. Flock.** 1994. Cloning and characterization of a gene for a 19 kDa fibrinogen-binding protein from *Staphylococcus aureus.* Mol. Microbiol. **12:**599–606.
5. **Bohach, G. A., and T. J. Foster.** 2000. *Staphylococcus aureus* exotoxins, p. 367–378. *In* V. A. Fischetti, R. P. Novick, J. J. Ferretti, D. A. Portnoy, and J. I. Rood (ed.), Gram-positive pathogens. ASM Press, Washington, D.C.
6. **Borst, D. W., and M. J. Betley.** 1993. Mutations in the promoter spacer region and early transcribed region increase expression of staphylococcal enterotoxin A. Infect. Immun. **61:**5421–5425.
7. **Borst, D. W., and M. J. Betley.** 1994. Phage-associated differences in staphylococcal enterotoxin A gene (*sea*) expression correlate with *sea* allele class. Infect. Immun. **62:**113–118.
8. **Borst, D. W., and M. J. Betley.** 1994. Promoter analysis of the staphylococcal enterotoxin A gene. J. Biol. Chem. **269:**1883–1888.
9. **Boyd, E. F., and H. Brussow.** 2002. Common themes among bacteriophage-encoded virulence factors and diversity among the bacteriophages involved. Trends Microbiol. **10:**521–529.
10. **Broudy, T. B., V. Pancholi, and V. A. Fischetti.** 2002. The in vitro interaction of *Streptococcus pyogenes* with human pharyngeal cells induces a phage-encoded extracellular DNase. Infect. Immun. **70:**2805–2811.
11. **Broudy, T. B., V. Pancholi, and V. A. Fischetti.** 2001. Induction of lysogenic bacteriophage and phage-associated toxin from group A streptococci during coculture with human pharyngeal cells. Infect. Immun. **69:**1440–1443.
12. **Bruckner, R.** 1997. Gene replacement in *Staphylococcus carnosus* and *Staphylococcus xylosus.* FEMS Microbiol. Lett. **151:**1–8.
13. **Carroll, D., M. A. Kehoe, D. Cavanagh, and D. C. Coleman.** 1995. Novel organization of the site-specific integration and excision recombination functions of the *Staphylococcus aureus* serotype F virulence-converting phages ϕ13 and ϕ42. Mol. Microbiol. **16:**877–893.
14. **Coleman, D. C., D. J. Sullivan, R. J. Russell, J. P. Arbuthnott, B. F. Carey, and H. M. Pomeroy.** 1989. *Staphylococcus aureus* bacteriophages mediating the simultaneous lysogenic conversion of beta-lysin, staphylokinase and enterotoxin A: molecular mechanism of triple conversion. J. Gen. Microbiol. **135:**1679–1697.
15. **Cortes, G., B. de Astorza, V. J. Benedi, and S. Alberti.** 2002. Role of the *htrA* gene in *Klebsiella pneumoniae* virulence. Infect. Immun. **70:**4772–4776.
16. **Crutz-Le Coq, A. M., B. Cesselin, J. Commissaire, and J. Anba.** 2002. Sequence analysis of the lactococcal bacteriophage bIL170: insights into structural proteins and HNH endonucleases in dairy phages. Microbiology **148:**985–1001.
17. **Dinges, M. M., P. M. Orwin, and P. M. Schlievert.** 2000. Exotoxins of *Staphylococcus aureus.* Clin. Microbiol. Rev. **13:**16–34.
18. **Dodd, I. B., and J. B. Egan.** 1990. Improved detection of helix-turn-helix DNA-binding motifs in protein sequences. Nucleic Acids Res. **18:**5019–5026.
19. **Freeman, V.** 1951. Studies on the virulence of bacteriophage-infected strains of *Corynebacterium diphtheriae.* J. Bacteriol. **61:**675–688.
20. **Hendrix, R. W., M. C. Smith, R. N. Burns, M. E. Ford, and G. F. Hatfull.** 1999. Evolutionary relationships among diverse bacteriophages and prophages: all the world's a phage. Proc. Natl. Acad. Sci. USA **96:**2192–2197.
21. **Hook, M. F., and T. J. Foster.** 2000. Staphylococcal surface proteins, p. 386–391. *In* V. A. Fischetti, R. P. Novick, J. J. Ferretti, D. A. Portnoy, and J. I. Rood (ed.), Gram-positive pathogens. ASM Press, Washington, D.C.
22. **Iandolo, J. J., V. Worrell, K. H. Groicher, Y. Qian, R. Tian, S. Kenton, A. Dorman, H. Ji, S. Lin, P. Loh, S. Qi, H. Zhu, and B. A. Roe.** 2002. Comparative analysis of the genomes of the temperate bacteriophages ϕ11, ϕ12 and ϕ13 of *Staphylococcus aureus* 8325. Gene **289:**109–118.
23. **Ikebe, T., A. Wada, Y. Inagaki, K. Sugama, R. Suzuki, D. Tanaka, A. Tamaru, Y. Fujinaga, Y. Abe, Y. Shimizu, H. Watanabe, and the Working Group for Group A Streptococci in Japan.** 2002. Dissemination of the phage-associated novel superantigen gene *speL* in recent invasive and noninvasive *Streptococcus pyogenes* M3/T3 isolates in Japan. Infect. Immun. **70:**3227–3233.
24. **Kaneko, J., T. Kimura, S. Narita, T. Tomita, and Y. Kamio.** 1998. Complete

nucleotide sequence and molecular characterization of the temperate staphylococcal bacteriophage ϕPVL carrying Panton-Valentine leukocidin genes. Gene **215:**57–67.

25. **Kondo, I., and K. Fujise.** 1977. Serotype B staphylococcal bacteriophage singly converting staphylokinase. Infect. Immun. **18:**266–272.
26. **Kreiswirth, B. N., S. Lofdahl, M. J. Betley, M. O'Reilly, P. M. Schlievert, M. S. Bergdoll, and R. P. Novick.** 1983. The toxic shock syndrome exotoxin structural gene is not detectably transmitted by a prophage. Nature **305:**709–712.
27. **Kuroda, M., T. Ohta, I. Uchiyama, T. Baba, H. Yuzawa, I. Kobayashi, L. Cui, A. Oguchi, K. Aoki, Y. Nagai, J. Lian, T. Ito, M. Kanamori, H. Matsumaru, A. Maruyama, H. Murakami, A. Hosoyama, Y. Mizutani-Ui, N. K. Takahashi, T. Sawano, R. Inoue, C. Kaito, K. Sekimizu, H. Hirakawa, S. Kuhara, S. Goto, J. Yabuzaki, M. Kanehisa, A. Yamashita, K. Oshima, K. Furuya, C. Yoshino, T. Shiba, M. Hattori, N. Ogasawara, H. Hayashi, and K. Hiramatsu.** 2001. Whole genome sequencing of methicillin-resistant *Staphylococcus aureus.* Lancet **357:**1225–1240.
28. **Lee, J. C.** 1995. Electrotransformation of staphylococci. Methods Mol. Biol. **47:**209–216.
29. **Le Marrec, C., D. van Sinderen, L. Walsh, E. Stanley, E. Vlegels, S. Moineau, P. Heinze, G. Fitzgerald, and B. Fayard.** 1997. Two groups of bacteriophages infecting *Streptococcus thermophilus* can be distinguished on the basis of mode of packaging and genetic determinants for major structural proteins. Appl. Environ. Microbiol. **63:**3246–3253.
30. **Lunde, M., J. M. Blatny, D. Lillehaug, A. H. Aastveit, and I. F. Nes.** 2003. Use of real-time quantitative PCR for the analysis of ϕLC3 prophage stability in lactococci. Appl. Environ. Microbiol. **69:**41–48.
31. **Marsin, S., S. McGovern, S. D. Ehrlich, C. Bruand, and P. Polard.** 2001. Early steps of *Bacillus subtilis* primosome assembly. J. Biol. Chem. **276:**45818–45825.
32. **Missich, R., F. Weise, S. Chai, R. Lurz, X. Pedre, and J. C. Alonso.** 1997. The replisome organizer (G38P) of *Bacillus subtilis* bacteriophage SPP1 forms specialized nucleoprotein complexes with two discrete distant regions of the SPP1 genome. J. Mol. Biol. **270:**50–64.
33. **Narita, S., J. Kaneko, J. Chiba, Y. Piemont, S. Jarraud, J. Etienne, and Y. Kamio.** 2001. Phage conversion of Panton-Valentine leukocidin in *Staphylococcus aureus*: molecular analysis of a PVL-converting phage, ϕSLT. Gene **268:**195–206.
34. **Novick, R. P.** 1991. Genetic systems in staphylococci. Methods Enzymol. **204:**587–636.
35. **Novick, R. P.** 2003. Mobile genetic elements and bacterial toxinoses: the superantigen-encoding pathogenicity islands of *Staphylococcus aureus.* Plasmid **49:**93–105.
36. **Novick, R. P.** 2000. Pathogenicity factors and their regulation, p. 392–407. *In* V. A. Fischetti, R. P. Novick, J. J. Ferretti, D. A. Portnoy, and J. I. Rood (ed.), Gram-positive pathogens. ASM Press, Washington, D.C.
37. **Pallen, M. J., and B. W. Wren.** 1997. The HtrA family of serine proteases. Mol. Microbiol. **26:**209–221.
38. **Pedre, X., F. Weise, S. Chai, G. Luder, and J. C. Alonso.** 1994. Analysis of cis and trans acting elements required for the initiation of DNA replication in the *Bacillus subtilis* bacteriophage SPP1. J. Mol. Biol. **236:**1324–1340.
39. **Ptashne, M.** 1992. A genetic switch. Cell Press, Cambridge, Mass.
40. **Ramirez, E., M. Schmidt, U. Rinas, and A. Villaverde.** 1999. RecA-dependent viral burst in bacterial colonies during the entry into stationary phase. FEMS Microbiol. Lett. **170:**313–317.
41. **Schlievert, P. M.** 1993. Role of superantigens in human disease. J. Infect. Dis. **167:**997–1002.
42. **Steinberg, J. P., C. C. Clark, and B. O. Hackman.** 1996. Nosocomial and community-acquired *Staphylococcus aureus* bacteremias from 1980 to 1993: impact of intravascular devices and methicillin resistance. Clin. Infect. Dis. **23:**255–259.
43. **Voyich, J. M., D. E. Sturdevant, K. R. Braughton, S. D. Kobayashi, B. Lei, K. Virtaneva, D. W. Dorward, J. M. Musser, and F. R. DeLeo.** 2003. Genome-wide protective response used by group A streptococcus to evade destruction by human polymorphonuclear leukocytes. Proc. Natl. Acad. Sci. USA **100:**1996–2001.
44. **Wagner, P. L., M. N. Neely, X. Zhang, D. W. Acheson, M. K. Waldor, and D. I. Friedman.** 2001. Role for a phage promoter in Shiga toxin 2 expression from a pathogenic *Escherichia coli* strain. J. Bacteriol. **183:**2081–2085.
45. **Wagner, P. L., and M. K. Waldor.** 2002. Bacteriophage control of bacterial virulence. Infect. Immun. **70:**3985–3993.
46. **Waldor, M. K., and J. J. Mekalanos.** 1996. Lysogenic conversion by a filamentous phage encoding cholera toxin. Science **272:**1910–1914.
47. **Yamaguchi, T., T. Hayashi, H. Takami, K. Nakasone, M. Ohnishi, K. Nakayama, S. Yamada, H. Komatsuzawa, and M. Sugai.** 2000. Phage conversion of exfoliative toxin A production in *Staphylococcus aureus.* Mol. Microbiol. **38:**694–705.
48. **Yarwood, J. M., J. K. McCormick, M. L. Paustian, P. M. Orwin, V. Kapur, and P. M. Schlievert.** 2002. Characterization and expression analysis of *Staphylococcus aureus* pathogenicity island 3. Implications for the evolution of staphylococcal pathogenicity islands. J. Biol. Chem. **277:**13138–13147.
49. **Ye, Z. H., and C. Y. Lee.** 1993. Cloning, sequencing, and genetic characterization of regulatory genes, *rinA* and *rinB*, required for the activation of staphylococcal phage ϕ11 *int* expression. J. Bacteriol. **175:**1095–1102.